

$S=2$ antiferromagnetic quantum spin chain

Ulrich Schollwöck, Olivier Golinelli, and Thierry Jolicœur
Service de Physique Théorique, CEA Saclay, F-91191 Gif-sur-Yvette, France
 (Received 13 November 1995; revised manuscript received 22 April 1996)

We have investigated Haldane's conjecture for the $S=2$ antiferromagnetic quantum spin chain with nearest-neighbor exchange J . Using a density matrix renormalization group algorithm for chains up to $L=350$ spins, we find in the thermodynamic limit a finite gap of $\Delta=0.085(5)J$ and a finite spin-spin correlation length $\xi=49(1)$ lattice spacings. We have confirmed the gap value by a zero-temperature quantum Monte Carlo study. We show that the ground state has a hidden topological order that is revealed in a nonlocal string correlation function which saturates to a nonzero value in the thermodynamic limit. We investigate the behavior of the spin-2 chain under an easy-plane anisotropy $D(S_i^z)^2$, $D>0$, and find that the Haldane and the large- D phase are separated by an XY phase. The string correlation function vanishes only in the $D\rightarrow\infty$ limit and does not distinguish between the Haldane phase and the perturbative large- D phase. An analysis of the transition mechanism and of the $S=2$ phase diagram in the presence of easy-plane and exchange anisotropy, markedly different from the $S=1$ phase diagram, allow us to conjecture how the classical limit is reached from increasing integer spins. [S0163-1829(96)00430-4]

I. INTRODUCTION

Interest in one-dimensional quantum spin chains has greatly increased in the last decade, after Haldane's conjecture¹ that the physical properties of antiferromagnetic quantum spin chains depend crucially on whether the spin is integer or half-integer. This challenged the conventional wisdom that the properties of these chains were generically given by the Bethe Ansatz solution of the spin-1/2 chain, which has a gapless excitation spectrum and an infinite correlation length. Haldane's prediction of a ground state with a finite spin-spin correlation length and a finite gap to spin excitations for integer quantum spin chains has been studied in numerous works. Numerical methods have served to establish quantitative results where analytical work had to rely on often uncontrolled approximations. Both the existence of a finite gap between a ground state singlet and excited states (called Δ_S for a generic spin value S and Δ in the $S=1$ case) and of a finite correlation length are well established for the $S=1$ isotropic antiferromagnetic quantum spin chain.²⁻⁶ The correlation length is $\xi\approx 6$ lattice spacings and the gap is $\approx 0.41J$ for the nearest-neighbor isotropic Heisenberg chain with exchange J (in the following, we measure energies in units of J and distances in lattice spacings). The spin wave velocity is $c=\Delta\xi=2.475(5)$, to be compared to the semiclassical value $c=2S=2$. The Haldane phenomenon is known⁷ to happen also in a general class of integer spin chain Hamiltonians, the so-called valence-bond-solid (VBS) Hamiltonians, with a simple ground state, a finite correlation length, as well as a gap to spin excitations. They moreover show no magnetic order, but a form of hidden topological long-range order, which is well understood⁸⁻¹⁰ for $S=1$. In the case of the spin-1 chain it is well established by now that the VBS Hamiltonian is close to the Heisenberg Hamiltonian in the sense that it qualitatively captures all relevant physical features of the Heisenberg chain. It is therefore also interesting to investigate whether this generic behavior is also ob-

served for the $S=2$ chain. If so, many physical properties of the $S=2$ chain could be at least qualitatively understood and the claim that the VBS Hamiltonian and the Heisenberg Hamiltonian are generically the same for all S further supported. Due to the asymptotic form¹ $\Delta_S\approx S^2\exp(-\pi S)$, the investigation of the $S=2$ case is hindered by the fact that one expects $\Delta_{S=2}\ll\Delta_{S=1}$ and $\xi_{S=2}\gg\xi_{S=1}$. One may guess $\Delta_{S=2}\approx 0.07$ and $\xi_{S=2}\approx 70$. The much larger correlation length makes finite size extrapolations feasible only for much longer chains than in the $S=1$ case; furthermore, the inherent statistical or systematical imprecisions of all numerical methods become more worrisome due to the small size of the gap. At the same time, the number of states per site rises from three to five, greatly reducing the length of numerically tractable chains. To our knowledge, the largest chains treated by exact diagonalization¹¹ had length 12.

We have used an implementation of the density matrix renormalization group (DMRG) that is described in Sec. II. Our estimates for the Haldane gap and ground state energy are contained in Sec. III. These are confirmed by a zero-temperature quantum Monte Carlo in Sec. IV. The spin correlation length is studied in Sec. V. In Sec. VI, we discuss the hidden topological order as well as the effect of anisotropies, single-ion and exchange anisotropy: we investigate the expected transition to a large- D phase under the introduction of a single-ion easy-plane anisotropy $D(S_i^z)^2$, $D>0$. We find that the string correlation function that reveals the nonlocal order vanishes only in the limit $D\rightarrow\infty$ and therefore is not a useful order parameter to discriminate between the Haldane and the large- D phase. Our conclusions are given in Sec. VI. We show that Haldane's conjecture is obeyed: the Haldane gap also exists for $S=2$, further supporting that the gap exists for all integer spins. Our results for the correlation length and the spin wave velocity also fit Haldane's picture of the integer spin chain. We establish the nonzero expectation value of a string correlation function in the thermodynamic limit. Contrary to $S=1$, the Haldane and large- D phases are

not separated by a transition point, but a whole critical phase. Our results indicate that this is generic for all $S \geq 2$ and $S=1$ thus a special case. The critical phase seems to replace both the Haldane phase and the large- D phase for $S \rightarrow \infty$, smoothly recovering the classical limit. We find no evidence of a cascade of S phase transitions, as proposed by Ref. 12. Investigating the $S=2$ phase diagram in the presence of an easy plane and an exchange anisotropy, we find for $S=2$ a phase diagram close to the classical limit, but substantially different from the $S=1$ case. We conjecture therefore that the $S=2$ case is generic for integer spin chains, whereas the $S=1$ case is special. Some of these results appeared already in a letter.¹³

II. THE DMRG METHOD

The choice of the density matrix renormalization group algorithm was determined by the fact that this method allows one to treat very long chains by comparison to exact diagonalization methods while retaining good precision for energies and expectation values. The DMRG is however special in that it contains a number of free parameters which have to be chosen carefully to obtain the desired accuracy at reasonable computational cost and to get a satisfying estimate of the precision actually obtained. We do not aim at a complete description of the DMRG; for this the reader is referred to Refs. 14 and 15. This method is extremely successful in the $S=1$ case.¹⁶ We will just briefly outline the method and highlight the available fine-tuning parameters which we will have to consider in the calculations that follow.

We consider the following general one-dimensional problem: a short-range interaction Hamiltonian H on a chain of length L with N states per site and arbitrary boundary conditions. The low-temperature (especially $T=0$) physics will be well captured by the ground state and the lowest excited states. These can be obtained by diagonalizing a matrix of size N^L using techniques like the Lanczos iterative diagonalization algorithm. The tractable chain lengths are severely limited by the geometrical increase of the matrix size. The DMRG surmounts this difficulty by diagonalizing chains of linearly increasing length, until the desired system size is reached, while retaining only a fixed number M of states out of the growing Hilbert space after each diagonalization, thus treating an approximate system. In the standard version, chains are composed out of a left block of spins, which is described by M states, two spins in the center, and a right block of spins. This hybrid system is diagonalized, or more precisely speaking, the targeted state (ground state, first excited state) determined. Two new blocks are now formed from the old blocks plus the adjacent site. The new block has initially MN states, of which M states are retained. The M states to be retained are those which contribute most to the projection of the targeted state on the new block, i.e., the eigenvectors of the reduced density matrix obtained from this projection belonging to the M largest eigenvalues of the reduced density matrix. As $\sum_{i=1}^{MN} \lambda_i = 1$, the truncation error $1 - \sum_{i=1}^M \lambda_i$ is a good measure of the precision of the results: it tells us how much of the projection of the targeted state we are losing by the truncation. We find a proportionality between errors in chain energies and the truncation error. For other quantities, the connection is more intricate. The next

chain is formed from the new blocks and two sites added in the center, thus $L \rightarrow L+2$, and the procedure repeated. After the chain has grown to the desired length, one may calculate expectation values of observables relative to the targeted state, for which purpose one has to keep matrix elements of the desired observables in the basis of the truncated Hilbert space, which have to be updated at each truncation.

We want to outline three major problems that one may encounter in the application of the DMRG: The system considered is an open system, which, while interesting in its own respect, leads a slower convergence to the bulk limit contrary to a periodic chain. As has been shown in Ref. 14, periodic (in general closed) systems are tractable, but the precision obtained is largely inferior. Manipulating the exchange couplings at the chain ends while retaining the bulk couplings may change the open boundary conditions such that certain properties of systems with periodic boundary conditions are mimicked. This is not in general straightforward: some physical properties are strongly dependent on the coupling strengths at the chain ends.

Another problem is that the choice of the states to be kept using the reduced density matrix is, in a certain sense, optimal for the chain that has just been diagonalized. However, what one really wants are those states that give the maximum contribution to the chain of the next iteration, which is slightly longer. The states chosen are just the most probable ones if we rely on the assumption that the projection of a chain state on a subsection of the chain (a block) does not depend crucially on small variations of the total chain length. This is certainly well obeyed for long chains, but not for the short chains at the beginning of the growth. We therefore accumulate errors coming from ‘‘bad’’ truncations at the beginning of the buildup. White¹⁴ has given a solution to this problem, which is to let a chain grow to its full size, and then to recalculate the small blocks of the beginning of the growth process, using the (approximative) knowledge on the total system. As we are working in a long system now, this procedure will give better truncations, and lead to new predictions for the total system. These, in turn, can again be used to ameliorate the description of the blocks. This process is time expensive, and we will have to investigate whether it is necessary to iterate, and after how many iterations the return-on-investment, precision for time, will still be worthwhile.

Furthermore, the errors introduced by the DMRG have a systematic, not statistical, character. While this is useful to give error estimates and control the algorithm, this may lead to serious problems, if results are not extrapolated carefully: unless the precision obtained is such that numerical results for a given M are more or less the exact ones, it is not correct to extrapolate results in L for a given M : the systematic errors may introduce artefacts into the convergence behavior which may be difficult to separate from the real convergence behavior (an example will be given below). It is therefore in general necessary to extrapolate first carefully in M to $M = \infty$ (equivalent to the exact result) and only then in L to $L = \infty$. We have thus decided to perform a quantum Monte Carlo study as discussed in Sec. IV: there are also systematic errors in this method but they are completely different. Compatibility of the results is expected to be a good check of the error control.

III. THE HALDANE GAP FOR $S=2$

A. Choice of the end couplings

Throughout this study we are guided by the so-called valence-bond-solid (VBS) wave functions.⁷ They are exact ground states of very special spin Hamiltonians:

$$H_{\text{VBS}} = \sum_{i=1}^{L-1} \sum_{k=S+1}^{2S} \alpha_k P_k(\mathbf{S}_i + \mathbf{S}_{i+1}), \quad (1)$$

where P_k is the projector on the $\mathbf{S}^2 = k(k+1)$ subspace and $\alpha_k > 0$. For $S=2$, the VBS Hamiltonian reads explicitly

$$\begin{aligned} H_{\text{VBS}}(\alpha_3, \alpha_4) = & \sum_{i=1}^{L-1} [(\alpha_3 + \alpha_4)(\mathbf{S}_i \cdot \mathbf{S}_{i+1})^4 + (10\alpha_3 + 14\alpha_4) \\ & \times (\mathbf{S}_i \cdot \mathbf{S}_{i+1})^3 + (7\alpha_3 + 63\alpha_4)(\mathbf{S}_i \cdot \mathbf{S}_{i+1})^2 \\ & + (-162\alpha_3 + 90\alpha_4)(\mathbf{S}_i \cdot \mathbf{S}_{i+1}) - 360\alpha_3]. \end{aligned} \quad (2)$$

The ground state can be constructed by replacing each spin S by $2S$ symmetrized spin-1/2 and S singlet links going to each neighboring site, linking two spin 1/2 each. In this exactly solvable model, all correlations can be calculated: One finds¹⁷ a correlation length $\xi = (\ln 3)^{-1} \approx 0.91$ for $S=1$ and $\xi = (\ln 2)^{-1} \approx 1.44$ for $S=2$. It is clear from this picture that in an open chain there are S free spin-1/2 on each end, leading to an effective free spin $S/2$ on each end of the chain. There is an effective interaction between these free spins, which vanishes in the limit $L \rightarrow \infty$. We are therefore left with an $(S+1)^2$ -fold degenerate ground state in the thermodynamic limit.

The Haldane gap is properly defined as the energy gap between the ground state and the first excited state of a periodic chain in the thermodynamic limit, where the ground state is not degenerate. For the open $S=2$ VBS Hamiltonian, it is the gap between the manifolds of $S=2$ and $S=3$ states. In the following we will assume that the essential physics of the $S=2$ Heisenberg Hamiltonian is captured by the $S=2$ VBS Hamiltonian described in the last section and show that a consistent picture emerges. Following White and Huse,¹⁵ we pick one state out of the manifold created by the free end spins, by adding a spin $S/2$ to each chain end and coupling them antiferromagnetically to the chain. We consider an open $S=2$ chain with a spin 1 at each end ($S_1 = S_L = 1$, $S_i = 2$ otherwise):

$$H = J_{\text{end}} \mathbf{S}_1 \cdot \mathbf{S}_2 + J \sum_{i=2}^{L-2} \mathbf{S}_i \cdot \mathbf{S}_{i+1} + J_{\text{end}} \mathbf{S}_{L-1} \cdot \mathbf{S}_L. \quad (3)$$

The degeneracy is lifted if the end coupling J_{end} exceeds a critical value $\approx \Delta_S/S$: If the coupling is below this value, the lowest excitation is obtained by exciting one end bond into its triplet state, which costs $J_{\text{end}}S$ energy. The excitation is then localized in the ends. To obtain the bulk excitation, which costs an energy Δ_S , the end state excitation must be energetically disfavored.

One still has to find a suitable J_{end} in the allowed regime. We have investigated $0.2 < J_{\text{end}} < 2.5$, considering chains up to length $L=90$ and keeping $M=90$ states. We find that for all J_{end} considered, the gap curves (energy difference be-

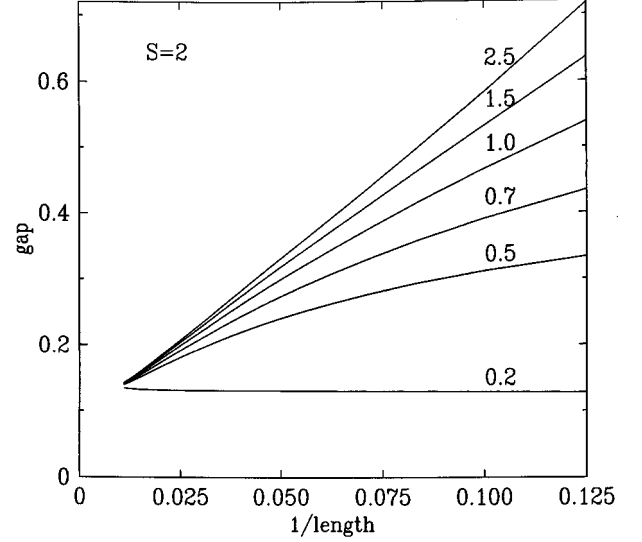


FIG. 1. Gap behavior for the $S=2$ chain with spin-1 ends and various end couplings J_{end} . All curves were calculated with $M=90$ states. The small curvature upwards for $L \rightarrow 90$ is an artifact (see text). The label on the right is the value of J_{end} .

tween the ground states in the $S_{\text{total}}^z = 0$ and $S_{\text{total}}^z = 1$ subspaces) decrease and converge towards each other for $L \rightarrow \infty$; all J_{end} are well beyond the expected bulk-to-edge excitation crossover value of $J_{\text{end}} \approx 0.05$ (Fig. 1) and the first excitation for very long chains clearly independent of J_{end} . There is a small deflection of the gap curve towards larger values, which is barely noticeable for $L \rightarrow 90$ for $J_{\text{end}} \geq 0.5$ and obvious for $J_{\text{end}} = 0.2$: this is an artefact of the DMRG due to the lack of extrapolation in M . At least for $0.5 \leq J_{\text{end}} \leq 2.5$, where the truncation errors are very close (see below), this artefact leads to the same overestimation of the gap (≈ 0.01 for $L=90$) for all J_{end} , which is why we did not extrapolate to remove the small artefact. For $J_{\text{end}} = 0.2$, the error is ≈ 0.02 .

This ensures that the gap we are calculating is a bulk property of the chain and does not depend on the manipulations of the chain ends. The corresponding diagram for $S=1$ is given in Fig. 2 where we established the crossover value to be $J_{\text{end}} \approx 0.5$: above the critical coupling, all gap curves meet (as the correlation length for $S=1$ is much smaller than for $S=2$, the convergence is faster). Below the critical coupling, the gap increases for increasing L and saturates to a value $\Delta \approx J_{\text{end}}$, as expected.

Our choice of J_{end} for the high-precision calculations is determined by two competing factors, the faster convergence to the limiting gap value for $L \rightarrow \infty$ for small J_{end} , and a substantial increase in the truncation error $P(M) = (1 - \sum_{i=1}^M \lambda_i)$ for small J_{end} . To understand these competing factors, we consider the ‘‘local gap’’ defined as $\Delta_i = J_i [\langle \mathbf{S}_i \cdot \mathbf{S}_{i+1} \rangle_{\text{exc}} - \langle \mathbf{S}_i \cdot \mathbf{S}_{i+1} \rangle_{\text{gs}}]$, the difference in the local bond energies for the first excited and the ground state. Obviously $\Delta = \sum_i \Delta_i$. In Fig. 3, we show $(\Delta_i + \Delta_{i+1})/2$ (to reduce dimerization effects discussed below) for different J_{end} in a chain of length 90. In a periodic system, the distribution of the gap energy would be uniform. Here, for increasing J_{end} the gap energy is more and more localized in the center of the chain, as exciting the end bonds costs in-

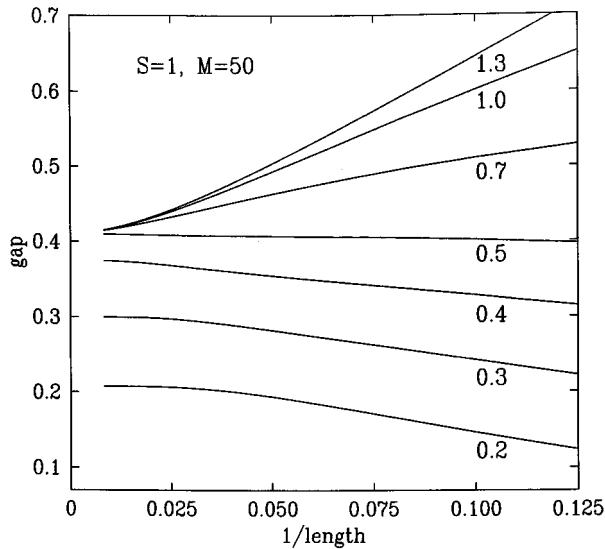


FIG. 2. Gap behavior for the $S=1$ chain with spin-1/2 ends and end couplings J_{end} . All curves were calculated with $M=50$ states. Note the different gap behavior depending on whether J_{end} is smaller or bigger than a critical $J_{\text{end}} \approx 0.51$. The label on the right is the value of J_{end} .

creasing energy. This argument is valid only for not too big J_{end} : For $J_{\text{end}} \rightarrow \infty$ the two end spins at each end will form an unexcitable singlet, and we are effectively left with a chain shortened by two sites and $J_{\text{end}}=1$. There is thus a limit to localization. Our results seem to indicate that the picture for $J_{\text{end}}=1$ and for $J_{\text{end}}=2.5$ is very similar and the limit thus attained. We mention that the central dip in the averaged gap energy is not physical, but an artefact of the DMRG: The effect is of the order $< 10^{-4}$ and only visible as the local gap energy is the small difference of two large energies, which

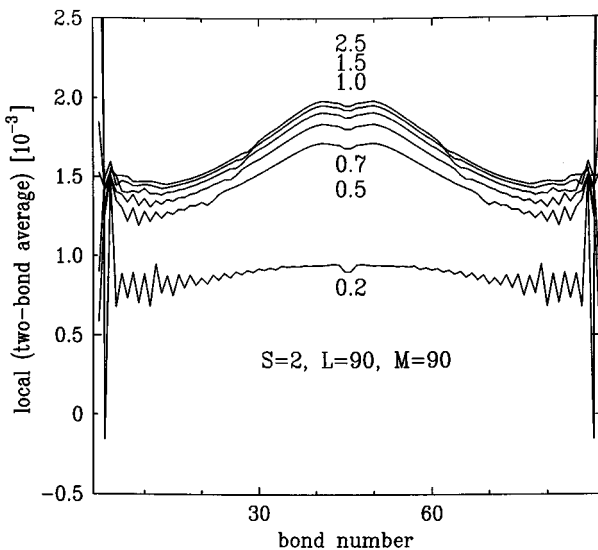


FIG. 3. Difference between the two-bond averaged bond energies for the first excited and the ground state (local gap) for different J_{end} . $M=90$ and $L=90$. Note the compression of the excitation for increasing J_{end} . The small central dip is an artefact due to the truncation errors of the DMRG and only visible due to the very small local gap. The central label is the value of J_{end} .

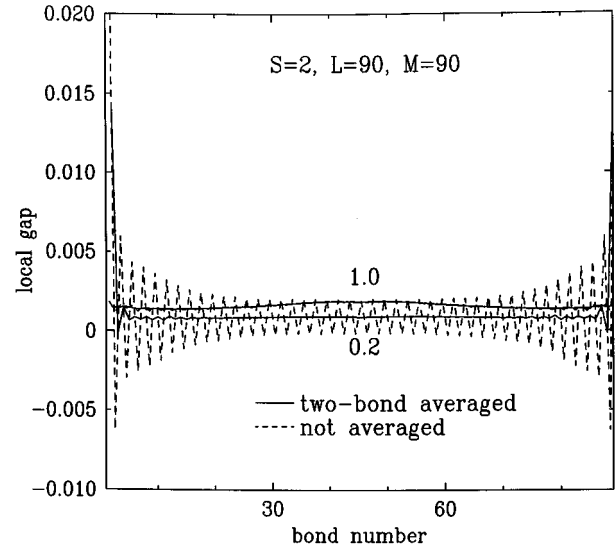


FIG. 4. Local gap energies as in Fig. 3, both two-site averaged (solid line) and unaveraged (dashed line). Observe the strong dimerization of the excitation for a small end coupling $J_{\text{end}}=0.2$.

themselves can be shown to be overestimated per bond by an order of 10^{-4} , where the error in the excitation energy is much larger. Bond energies in the chain center are calculated very precisely, as the bond is in the center of a long chain and no truncation occurs. The result is therefore extremely precise. Bond energies away from the center pick up the above error due to truncation effects, leading to an overestimation of the local gap of the order of the error. This is why systematically a dip is observed in the local gap energy. The dip is more pronounced for longer chains, where the local gap is smaller. By increasing M , it can be arbitrarily reduced.

In short chains, excitations of the end bonds are more important than in long chains and lead to the large discrepancies in the gap values for short chains. For weak end couplings, the excitation will be increasingly shifted towards the chain ends, which provide a hard boundary. This leads to a dimerization of the gap energy: in Fig. 4, we show the two-bond average of the local gap and the local gap for $J_{\text{end}}=1.0$ and $J_{\text{end}}=0.2$. For small couplings, there is a strong period of two in the local gap due to the boundary conditions: for $J_{\text{end}}=0.2$ the oscillation amplitude is about four times the local averaged gap, whereas it is negligible for $J_{\text{end}}=1$. Looking at the local bond energies, one sees that the dimerization is by far more important for the first excitation than for the ground state. The open boundary conditions, similar to a finite potential step, lead to a scattering of the excited state into other excited states, and thus a beat of period two.¹⁵ The problem of dimerization is that the bonds develop alternating character, implying that the truncation information obtained by creating a bond of type 1 is used to select states which will be used in the next step to build a bond of type 2 and the quality of truncation thus reduced. We effectively observe a steep increase in the truncation error $P(M)$ for the first excitation for small J_{end} in chains of length $L=90$, as given in Table I.

The effect on the truncation error for long chains is even worse, as the numbers given above are for a chain length

TABLE I. Truncation errors $P(M)$ as a function of the end coupling J_{end} for a chain of length $L=90$.

J_{end}	$P(M)$
2.5	0.52×10^{-5}
1.5	0.53×10^{-5}
1.0	0.54×10^{-5}
0.7	0.56×10^{-5}
0.5	0.59×10^{-5}
0.2	0.84×10^{-5}

$L=90$, where the truncation errors have not yet saturated to their infinite chain length value, and their difference is still increasing. A similar, but less pronounced, phenomenon can be observed for the ground states. As the error in the total energy is found to be proportional to $LP(M)$, even small increases in the truncation error severely limit the precision of the obtained gap values for large L , making extrapolations much more difficult. As the convergence of the various gap curves towards each other is fast, the choice in a region of, say, $0.7 \leq J_{\text{end}} \leq 1.5$, is basically free and we arbitrarily chose $J_{\text{end}}=1$, which seemed to us a reasonable compromise. In any case, the final outcome is not affected, apart from changes in the error estimate.

B. Energy estimates

We calculated the gap by subtraction of the energy of the lowest eigenstate in the $S_{\text{tot}}^z=0$ subspace, the true singlet ground state, from the energy of the lowest eigenstate in the $S_{\text{tot}}^z=1$ subspace, one of the states of the first excitation triplet. Due to the structure of the Hilbert space and the properties of the Lanczos algorithm the second eigenstate in the $S_{\text{tot}}^z=0$ subspace is only approximately degenerate with the first state in the $S_{\text{tot}}^z=1$ subspace, and always slightly higher in energy. We did not follow the approach of White and Huse for the spin-1 chain to make energy and spin density as uniform as possible in the center of a long spin chain and

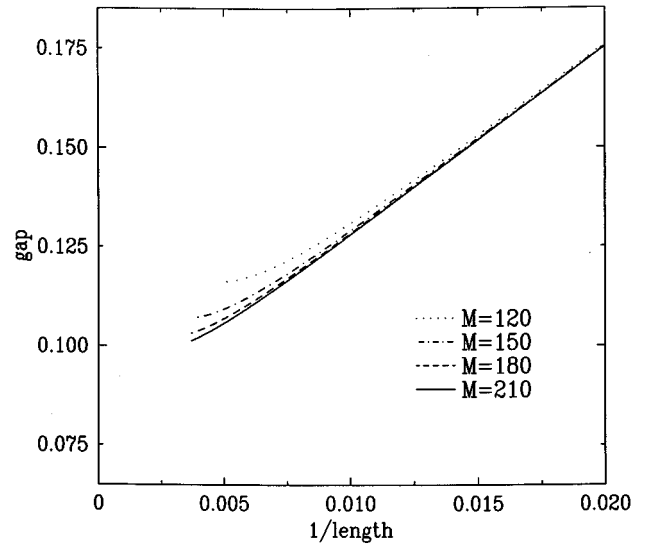


FIG. 5. Gap energies derived from uniterated energies of the ground and excited states for various M . Note the monotonic decrease of the gap with M and the deviation from an L^{-1} line which occurs later for larger M .

calculate the gap from this information. Their chains were typically of the order $L=100$; as we will find that for $S=2$ the correlation length increases by a factor of about 8, this means chains of the order $L=800$, beyond our possibilities.

To calculate the gap it is important to note that the unmodified infinite system algorithm given by White is *not* suitable to calculate the $S=2$ gap because of the truncation problem for short chains, and that extrapolations in M have to be done before extrapolations in L . In Fig. 5 we show the gap for a chain of length L taken from the difference of the two considered energies for fixed number M of kept states. It is obvious that for each M the gap curve becomes inflected away from an L^{-1} behavior at some point, and the gap seems to follow a parabolic curve. We will discuss later that one actually must expect such a gap behavior. Nevertheless we are only observing an artefact of the DMRG, which is

TABLE II. Gap values vs chain length L and kept states M . First line, results without iteration; second line, with iteration. Results for $M=\infty$ are obtained by extrapolation.

gap	$L=60$	$L=90$	$L=120$	$L=150$	$L=210$	$L=270$
$M=50$	0.1728					
	0.1616					
$M=70$	0.1655	0.1463				
	0.1609	0.1372				
$M=90$	0.1632	0.1412	0.1332	0.1314		
	0.1604	0.1352	0.1238	0.1183		
$M=120$	0.1606	0.1356	0.1244	0.1190	0.1162	
	—	0.1336	0.1209	0.1139	0.1076	
$M=150$	0.1600	0.1342	0.1217	0.1149	0.1087	0.1071
	—	—	0.1202	0.1127	0.1052	0.1020
$M=180$	0.1598	0.1336	0.1207	0.1134	0.1062	0.1033
	—	—	—	—	0.1040	0.1002
$M=210$	0.1597	0.1334	0.1203	0.1127	0.1049	0.1013
	—	—	—	—	—	0.0995
$M=\infty$	0.1597(1)	0.1333(1)	0.1202(1)	0.1124(2)	0.1034(3)	0.0985(5)

TABLE III. Ground state energies for $L=60,90,120$ vs M .

E_0	$L=60$	$L=90$	$L=120$
$M=50$	-277.363431	—	—
$M=70$	-277.370690	-420.205654	—
$M=90$	-277.372328	-420.208818	-563.045334
$M=120$	-277.322798	-420.209801	-563.046851
$M=150$	-277.372958	-420.210187	-563.047487
$M=180$	-277.372997	-420.210275	-563.047632
$M=210$	-277.373014	-420.210320	-563.047708

reduced for increasing M (i.e., increasing precision). The variational character of the method, which considers subspaces of the total Hilbert space, leads to a systematic overestimation of both energies considered, where for the first excitation the error is empirically found to be much more important: therefore, at each step, a finite *positive* error δ is added to the true gap. For long chains δ saturates. The accumulated gap error will first slow down the decrease of the gap and eventually lead to an increase in the calculated gap, when δ is larger than the decrease of the true gap for an increase in chain length. For an $S=1$ chain, this effect is of minor importance, as δ can be made extremely small for numerically manageable M , and can be ignored. This is, as shown in Fig. 5, not the case for $S=2$. We therefore had to use the much more time-consuming finite size algorithm, which reduces the effects of truncation errors and substantially diminishes δ . This algorithm can be in principle repeated *ad libitum*, but the corrections become rapidly very small and are outborn by numerical round-off errors. Investigating the iteration correction both for the ground state and the first excitation, we found that the most important contribution comes from the first iteration of the first excitation. All other corrections were typically at least a factor of 10 smaller and did not justify the computational effort. We therefore consider uniterated ground state energies and first excitation energies which have been iterated once. Our results indicate that the error δ is thus reduced by a factor of the order of 3, allowing one to treat, for a given desired precision, chains three times longer.

TABLE IV. Energy of the first excited state for $L=60,90,120$ vs M . First line, results without iteration; second line, with iteration.

E_1	$L=60$	$L=90$	$L=120$
$M=50$	-277.190606	—	—
	-277.201845	—	—
$M=70$	-277.205122	-420.059362	—
	-277.209792	-420.068504	—
$M=90$	-277.209163	-420.067665	-562.912119
	-277.211962	-420.073580	-562.921505
$M=120$	-277.212152	-420.074121	-562.922455
	—	-420.076194	-562.925939
$M=150$	-277.212918	-420.076014	-562.925787
	—	—	-562.927308
$M=180$	-277.213176	-420.076664	-562.926926
	—	—	—
$M=210$	-277.213283	-420.076953	-562.927456
	—	—	—

TABLE V. Ground state energies for $L=150,210,270$ vs M .

E_0	$L=150$	$L=210$	$L=270$
$M=90$	-705.881848	—	—
$M=120$	-705.883904	-991.558009	—
$M=150$	-705.884795	-991.559411	-1277.234028
$M=180$	-705.884999	-991.559735	-1277.234471
$M=210$	-705.885107	-991.559907	-1277.234707

We have calculated the gap for $L=60, 90, 120, 150, 210$, and 270 , retaining up to $M=210$ states. Our calculations were performed on a CRAY C94, reaching up to 180 MegaFlops for $M=210$. The calculation of the ground state properties for $L=270$ and $M=210$ took 10 322 sec of one CPU; calculation time was approximately linear in L and between quadratic and cubic in M . Memory usage was linear in L and quadratic in M . To extract the gap in the thermodynamic limit, we have to proceed in two steps: (i) For each L , the results are extrapolated to $M=\infty$, i.e., the exact gap for chain length L . (ii) The ‘exact’ results for each L are extrapolated to $L\rightarrow\infty$. In Table II, we give the gap results: in the first line, without iteration of the energy of the first excitation, in the second line, if calculated, with iteration of the energy of the first excitation.

The extrapolation in M is not carried out for the gap directly but for the energies. We find that for large L the energies can be well approximated by

$$E(M)=E+\alpha LP(M), \quad (4)$$

where $P(M)$ is the truncation error for the last step in the growth process of the chain. $P(M)$ decreases monotonically with M . We find α to be hardly dependent of L in the range considered and to be of the order 10 both for the ground state and the first excitation (the closeness of the two α is a pure coincidence). For the uniterated excitation energy, $\alpha\approx 30$. The energies found are given in Tables III–VI. The truncation error we find as in Table VII. E is then the extrapolation of the energy for $M\rightarrow\infty$ as $P(\infty)=0$.

The ground state energy results allow us to calculate the ground state energy per site E_0/L . Two effects have to be considered: first, the ground state energy per bond will converge to its bulk value only for sufficient $L\gg\xi$. This effect is

TABLE VI. Energy of the first excited state for $L=150,210,270$ vs M . First line, results without iteration; second line, with iteration.

E_1	$L=150$	$L=210$	$L=270$
$M=90$	-705.750495	—	—
	—	—	—
$M=120$	-705.764901	-991.441835	—
	-705.769971	-991.450422	—
$M=150$	-705.769910	-991.450671	-1277.126966
	-705.772093	-991.454243	-1277.132010
$M=180$	-705.771600	-991.453583	-1277.131213
	—	-991.455722	-1277.134216
$M=210$	-705.772409	-991.455040	-1277.234707
	—	—	-1277.135242

TABLE VII. Truncation errors for the last step as a function of L and M . First line, ground state; second line, first excited state. Digits in parenthesis give powers of 10.

$P(M)$	$L=60$	$L=90$	$L=120$	$L=150$	$L=210$	$L=270$
$M=50$	0.10(-4) 0...					
$M=70$	0.44(-5) 0.71(-5)	0.50(-5) 0.10(-4)				
$M=90$	0.13(-5) 0.35(-5)	0.16(-5) 0.54(-5)	0.17(-5) 0.69(-5)	0.18(-5) 0.80(-5)		
$M=120$	0.48(-6) 0.90(-6)	0.66(-6) 0.17(-5)	0.72(-6) 0.24(-5)	0.74(-6) 0.30(-5)	0.75(-6) 0.39(-5)	
$M=150$	0.15(-6) 0.30(-6)	0.23(-6) 0.60(-6)	0.26(-6) 0.88(-6)	0.28(-6) 0.11(-5)	0.29(-6) 0.15(-5)	0.29(-6) 0.18(-5)
$M=180$	0.71(-7) 0.13(-6)	0.12(-6) 0.28(-6)	0.14(-6) 0.43(-6)	0.15(-6) 0.56(-6)	0.16(-6) 0.76(-6)	0.16(-6) 0.92(-6)
$M=210$	0.37(-7) 0.67(-7)	0.64(-7) 0.15(-6)	0.81(-7) 0.24(-6)	0.92(-7) 0.32(-6)	0.94(-7) 0.44(-6)	0.94(-7) 0.53(-6)

enhanced by the open boundary conditions. Second, we will variationally overestimate the energy for finite M , with increasing precision with increasing M . We therefore first let the energy per bond for a given M converge in L ; these infinite-chain results are then extrapolated in M . We find that for $L \approx 120$ for each $M \leq 210$ considered the ground state energy per site has converged to a precision of 10^{-6} . Taking those energies as infinite-chain results, we find the results of Table VIII. The extrapolated result was again obtained from a linear dependence of the energies on the truncation error $P(M)$.

C. Gap estimate

To obtain now the gap in the thermodynamic limit, we can extrapolate our results for $90 \leq L \leq 270$ to $L = \infty$ by fitting an L^{-1} law (Fig. 1 of Ref. 13) and obtain a gap estimate of $0.081(1)$ for $L = \infty$. We note that deviations from perfect linear behavior are extremely small in the range of chain length we have considered. However it is important to note that the asymptotic behavior of the gap in an open chain is expected to be $1/L^2$: the massive quasiparticles have dispersion $E_k = \sqrt{\Delta_\infty^2 + c^2(k - \pi)^2} \approx \Delta_\infty + c^2(k - \pi)^2/2\Delta_\infty$ near the bottom of the band. On an open chain, the quasiparticle cannot stay in a stationary state with $k = \pi$ but instead $k - \pi \approx \pi/L$ as a particle in a box since there is no translational invariance. This means that the lowest excited state

TABLE VIII. Energies per bond for the isotropic $S=2$ chain and truncation errors as a function of M .

M	E_0/L	$P(M)$
90	-4.7612172	0.18×10^{-5}
120	-4.7612351	0.75×10^{-6}
150	-4.7612436	0.29×10^{-6}
180	-4.7612456	0.16×10^{-6}
210	-4.7612467	0.95×10^{-7}
∞	-4.761248(1)	—

has a gap $\Delta_\infty + c^2 \pi^2/2\Delta_\infty L^2 + O(1/L^3)$. This behavior has not yet been reached for $L=270$. Thus there must be a crossover point to parabolic behavior of $\Delta(L)$. As a consequence we can obtain an upper bound on the gap by assuming that the parabolic behavior sets in immediately beyond $L=270$. We match a parabolic curve $\Delta(L) = \Delta_\infty + aL^{-2}$ to our extrapolated linear gap curve at $L=270$ such that up to the first derivative the two regimes meet continuously. This leads to $\Delta_\infty = 0.090$ (and $a \approx 620$). We have also estimated the correlation length (see below) to be ≈ 50 and thus $c = \xi \Delta_\infty \approx 4.2$. This gives an estimate of the coefficient of the $1/L^2$ parabolic term. Using this estimate ($a_0 \approx 1024$) we now say that there is a crossover length L_0 at which asymptotic behaviour $\Delta(L) = \Delta_\infty + a_0/L^2$ sets in. Matching the parabolic curve to the straight line requires $\Delta_\infty = 0.085$ and $L_0 \approx 450$. This is a perfectly consistent set of results. We thus choose as a central value for the gap $\Delta_\infty = 0.085$ the lower bound being fixed by the linear fit of our data and the upper bound being 0.09 . We quote our final result as $\Delta = 0.085(5)$.

Our result, while in agreement with the estimate by Deisz *et al.*,¹⁸ deviates sensibly from the result given by Nishiyama *et al.*,¹⁹ who, from chains up to lengths $L \approx 70$ and $M \leq 110$ and assuming a L^{-1} behavior of the gap, give $\Delta = 0.055 \pm 0.015$. As the L^{-1} behavior is valid in the range of L they considered, we would expect that their result gives at least a lower boundary of the gap, which itself may be slightly higher than ours because of the small value of M . This is not the case. We expect that their approach to directly calculate the gap as the difference between the energies of the ground state and tenth excited state in an unmodified open chain without spin-1 sites at the end is too difficult for the DMRG for the M considered (due to computation time limits, we could not check what happens if we repeat their calculations with our code for greater M). As we observed “variational” behavior in all quantities we have considered, i.e., monotonous increase or decrease with M , we feel that the fact that their gap results do not show such behavior indicates problems in the application of the method.

IV. ZERO-TEMPERATURE QUANTUM MONTE CARLO STUDY

In this section, we present a study of the $S=2$ gap by a zero-temperature quantum Monte Carlo study. Here we describe shortly the Monte Carlo method; the reader can find more details in a previous article.²⁰ We think it is important to check the DMRG results by comparison with a totally different numerical method because it is difficult to know whether or not one controls the systematic errors.

We consider only the isotropic Heisenberg model for a *periodic* chain of N quantum spin 2:

$$H = \sum_{i=1}^L \vec{S}_i \cdot \vec{S}_{i+1}, \quad (5)$$

with $L+1 \equiv 1$. The symmetries are the conservation of total spin $\vec{S}_T = \sum_i \vec{S}_i$, the translation $i \rightarrow i+1$ and the reflection $i \rightarrow L-i$. In this section, only the conservation of $S_T^z = \sum_i S_i^z$ is explicitly used, but the quantum states generated are implicitly invariant by translation and reflection.

From a numerical point of view, H is a real, symmetric and sparse matrix, when expressed on the usual base $|\sigma\rangle = |s_1, \dots, s_L\rangle$ defined by $S_i^z |\sigma\rangle = s_i |\sigma\rangle$. The simplest method to compute the dominant eigenvalue is the *iteration* (or *power*) method: a initial vector V_0 is iterated by

$$H \cdot V_t = g(t) V_{t+1}, \quad (6)$$

where $g(t) = |H \cdot V_t|$ and the eigenvalue λ is given by $\lambda = \lim_{t \rightarrow \infty} g(t)$ with eigenvector $\lim_{t \rightarrow \infty} V_t$. We use the projection over an arbitrary vector Φ and $\lambda = \lim_{t \rightarrow \infty} (\Phi \cdot H \cdot V_t) / (\Phi \cdot V_t)$. With conserved symmetries, the matrix is block diagonal and the iteration method gives the dominant eigenvalue of the block containing the initial vector V_0 . For the integer spin chain, the ground state is a singlet $S_T=0$ and the first excitation is a triplet $S_T=1$. Then the gap is obtained from two runs with two different initial vectors : one with $S_T^z=0$ and one with $S_T^z=1$. For spin 2, exact results have been published^{11,21,22,4,23} for sizes up to $L=12$. By comparison, for spin 1, exact computations up to $L=22$ are possible.²⁴

The Monte Carlo method we use is the stochastic implementation of the direct iteration (6). It is a variant of the method of Nightingale and Blöte⁵ and an improvement on our previous work.²⁰ A general presentation of this kind of method is given in Ref. 25. It is a *zero-temperature* method because one obtains a representation of the ground state only, by opposition to the world-line Monte Carlo methods dealing with $\exp(-\beta H)$. Formally, in the iteration (6) the deterministic vector V_{t+1} is replaced by a stochastic one. We impose that Eq. (6) is now true in *average*:

$$H \cdot V_t = g(t) \langle V_{t+1} \rangle, \quad (7)$$

where $g(t)$ is a normalization factor and $\langle \cdot \rangle$ denotes the average over the stochastic step $V_t \rightarrow V_{t+1}$. This stochastic iteration is repeated several thousand times. When t is large, the sequences of V_t and $g(t)$ have a limiting probability distribution. The expectation values obtained by such a procedure are close but definitely not equal to the true ground

state Ψ_{gs} and its energy λ_{gs} . There is a systematic bias that has been studied in depth.^{26,27} Hetherington proposed the use of the following estimators :

$$\lambda(n) = \frac{\sum_t \Phi \cdot H \cdot V_{t+n} \cdot g(t+n-1) \cdots g(t+1) g(t)}{\sum_t \Phi \cdot V_{t+n} \cdot g(t+n-1) \cdots g(t+1) g(t)}, \quad (8)$$

where Φ is an arbitrary fixed vector. As the number of Monte Carlo steps t becomes large (n is fixed), both sums become equal to their averages over the limiting probability distribution of V_t . This average is denoted by $\langle \langle \cdot \rangle \rangle$. By using Eq. (7) n times

$$\lim_{t \rightarrow \infty} \lambda(n) = \frac{\Phi \cdot H^{n+1} \langle \langle V_t \rangle \rangle}{\Phi \cdot H^n \langle \langle V_t \rangle \rangle}. \quad (9)$$

This sequence of estimators ‘‘corrects’’ the systematic bias $\Psi_{gs} - \langle \langle V_t \rangle \rangle$ and

$$\lim_{n \rightarrow \infty} \lambda(n) = \lambda_{gs}. \quad (10)$$

By a similar formula the ground state Ψ_{gs} can be obtained.²⁶ The choice of the arbitrary vector Φ is very important. The variance (or fluctuations) and the bias are reduced if Φ is close to the true ground state Ψ_{gs} . We will choose it by minimization of a variational form, described in detail in Ref. 5. With this choice of Φ , the error bars are reduced by a factor of order 4 with respect to the projection onto the vector $\langle 1 |$ with all coordinates equal to one.

Many choices are possible for an algorithm which reproduces Eq. (7). In this work, the stochastic vector is a sum of W random ‘‘walkers’’ $|\sigma_r\rangle_{r=1,W}$ where $|\sigma_r\rangle$ is one of the basis state. The walkers evolve during the time and the elements of matrix H are considered as probability transition from a basis state to an another basis state. We refer the reader to Ref. 20, in which a precise description of the algorithm is given. The main difference with the implementation of Refs. 5, 25, 28, and 29 is the fact we keep the number of walkers constant during the time. In both cases (constant or fluctuating around a fixed target), correlations appear between walkers which are difficult to analyze.

To reduce fluctuations of V_t , it is very effective^{25,29} to use the representation H' of the Hamiltonian on the transformed basis $\Phi(\sigma)|\sigma\rangle$ where $\Phi(\sigma) = \langle \Phi | \sigma \rangle$, i.e., $H'(\sigma, \tau) = \Phi(\sigma) H(\sigma, \tau) \Phi(\tau)^{-1}$ where Φ is the variational approximation of the ground state described above. In other words, this transformation can be seen as the stochastic iteration of the initial matrix H but with weighted walkers $\Phi(\sigma_r)^{-1} |\sigma_r\rangle$. By this trick, we observe a reduction of the error bars by a factor of between 2 and 4. In this work, the weights $\Phi(\sigma)^{-1}$ depend only on the state σ , but in Refs. 25, 28, and 29, they are multiplied by another weighting process during the decimation phase of walkers. We are not convinced by the utility of this last trick and we do not use it. To estimate the standard deviation, several independent simulations were done. Then the independent results are averaged in the usual way.

We have used a Cray T3D parallel machine with 128 processors alpha. Each processor computes the evolution of a subset of walkers, and the processors with the most proliferating population give walkers to the processors with a poor

TABLE IX. Energy E_0 of the ground state $S=0$, E_1 of the first excitation $S=1$, energy per unit length E_0/L , and the gap value $E_1 - E_0$ for a periodic chain of L spins 2. The values for $L \leq 10$ are obtained by exact diagonalization; $N=12$ was published by Lin (Ref. 11); $L \geq 20$ are the results of Monte Carlo simulations. The standard error deviations are shown in parentheses.

L	E_0	E_1	E_0/L	Gap
4	-20.	-19.	-5.	1.0
6	-29.164693200754	-28.467398659937	-4.860782200126	0.697294540817
8	-38.521869135413	-37.976299855143	-4.815233641927	0.545569280270
10	-47.948445740133	-47.495220966136	-4.794844574013	0.453224773997
12	-57.40817	-57.01747	-4.784014	0.39070
20	-95.3754(4)	-95.1134(3)	-4.76877(2)	0.2620(5)
30	-142.927(1)	-142.7330(4)	-4.76423(3)	0.194(1)
50	-238.104(3)	-237.964(1)	-4.76208(6)	0.140(3)
80	-380.907(4)	-380.805(4)	-4.76134(5)	0.102(6)

population, in order to keep a balanced working. Our program written for an arbitrary value of the spin S and length L needs $L \times 2 \mu s$ by walker \times iteration. For the longest chain $L=80$, 21 independent samples with 186 880 walkers and 100 000 iterations were done in 120 h (i.e., 1.7 yr of single processors). We give in Table IX a compilation of exact results obtained for short chains and Monte Carlo results. The digits in parenthesis are the Monte Carlo fluctuations (one standard error deviation). The systematic errors (including the Hetherington bias) must be added.

The ground state energy E_0/L is determined with a good precision. Without extrapolation, one finds $E_0/L \approx -4.76$. A finite size extrapolation in $1/L^2$ is adequate, leading to $E_0/L = -4.7609(2)$. The digit in parenthesis represents only the Monte Carlo fluctuations and the error due to the extrapolation, but *not* the systematic bias. Our DMRG result is $E_0/L = -4.761248(1)$: this indicates a bias of order $+0.0003$ per bond, thus $+0.024$ for $L=80$. It is positive as shown in Ref. 27. It is clear that the DMRG is much more precise than the QMC.

The Haldane gap $G = E_1 - E_0$ is obtained by subtraction of two independent quantities. The absolute error ΔG is of the same order, but the relative error $\Delta G/G$ is bigger. For sizes less than 80, the behavior is $1/L$. Then the extrapolation gives $0.06(1)$. This value is slightly smaller than the DMRG result $0.085(5)$. One should consider that the extrapolation with a $1/N$ asymptotic law is a lower bound. The systematic bias is difficult to estimate. We conclude that there is no incompatibility between the DMRG and the Monte Carlo results.

V. CORRELATION FUNCTIONS IN THE $S=2$ QUANTUM SPIN CHAIN

To calculate the correlation length, we partially lift the ground state degeneracy of the open chain by adding a spin 1 on *one* end of the $S=2$ chain ($S_L = 1$; $S_i = 2$ otherwise):

$$H = J \sum_{i=1}^{L-2} \mathbf{S}_i \cdot \mathbf{S}_{i+1} + J_{\text{end}} \mathbf{S}_{L-1} \cdot \mathbf{S}_L. \quad (11)$$

The ground state will then be a spin 1 triplet; at the spin-2 end of the chain (position 1) one expects an effective free

spin 1. If we consider the ground state with $S_{\text{total}}^z = 1$, it is expected that $\langle S_i^z \rangle$ decays purely exponentially¹⁵ from a value around ± 1 :

$$\langle S_i^z \rangle \propto (-1)^{i-1} \exp[-(i-1)/\xi]. \quad (12)$$

We choose this approach, as from this equation, the correlation length ξ can be obtained much more precisely than from the decay of $C(|i-j|) = \langle \mathbf{S}_i \cdot \mathbf{S}_j \rangle$. This is because this approach partially suppresses systematic errors of the DMRG due to an effective fixed boundary condition (see below) and because there is a partial cancellation for errors, whereas they build up for the two-point correlations, as correlated states in each half-chain are systematically neglected at the same time, underestimating ξ . This was already shown by White and Huse:¹⁵ they calculated the correlation length for $S=1$ using both approaches, and showed that the results are equivalent. We assume that this is a generic property of spin- S chains which are in the same phase as the VBS-Hamiltonian. In the $S=1$ case this seems numerically directly established for ξ ; in the $S=2$ case, all results indicate that the spin-2 Heisenberg chain shares the properties of the VBS chain.

Though the $S=1$ chain is much less critical than the $S=2$ chain and the number M of states necessary to describe the excitation spectrum mediating the correlation much smaller, the conventional correlation length was found¹⁵ to be $\xi_{S=1} \approx 5.15$ for $M=48$ [and a truncation error $P(M) = 4.13 \times 10^{-9}$] and $\xi_{S=1} \approx 5.45$ for $M=110$ [$P(M) = 1.27 \times 10^{-11}$] as to be compared to the boundary correlation length $\xi = 6.03$, which itself is in good agreement with other estimates (whereas the smaller values are not). In our calculations, for $M=210$, we find $P(M) = 9.4 \times 10^{-8}$, which is much larger, and we must expect even worse results for $S=2$ using the conventional approach. To get an estimate, we have evaluated the correlation length from the decay of the spin-spin correlation using a chain of $L=270$ and $M=150$ [$P(M) = 2.9 \times 10^{-6}$], and found $\xi \approx 33$, which is a lower bound on the actual correlation length (and about 68% of the limiting value).

Computing now the correlation length using the spin-1 end approach, we have to perform an extrapolation of ξ with

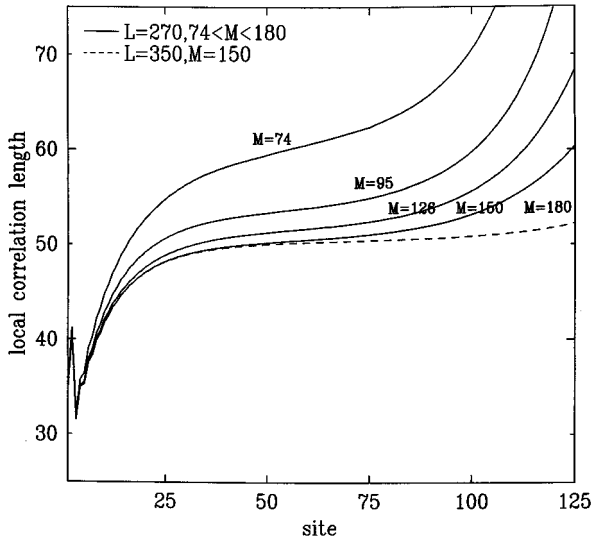


FIG. 6. Two-site average of the local correlation length $2/(\ln|\langle S_i^z \rangle| - \ln|\langle S_{i+2}^z \rangle|)$ vs site i for $i < 125$ for the same chain as in Fig. 2. The deviations from the shoulder in the center of the diagram are finite size and finite precision effects (for the right end).

respect to M because of the slow increase of precision with M for $S=2$. At the same time we consider chains of length $L=270$ and repeat some calculations for $L=350$, to study possible finite size effects. We find that those are minor, as are effects of the choice of J_{end} , and concentrate on the extrapolation in M . In Fig. 2 of Ref. 13, we give $\ln|\langle S_i^z \rangle|$ vs i . The generic behavior is the same for all M : After the expected decay of $|S^z|$, there is a small increase towards the other end of the chain (greatly exaggerated by the logarithmic scale). With increasing M , the minimum shifts to the right, the spin expectation value at the right end of the chain is greatly reduced, the decay becomes more exponential and approaches a limiting curve which we take to be the $M=\infty$ result. We do not know numerically whether the decay will become exponential over the total chain length. The $S=1$ case seems to indicate that with sufficient precision, i.e., very large M , this will be the case: there, for $M=90$, the decay is perfectly exponential to the end of the chain. It is worthwhile to retain that here we have a case where the same quantity is determined with very variable precision depending on the site, and where reliance on a small truncation error may be entirely misleading: the error has, in our analysis, the following source: The ground state we are considering has effectively fixed boundary conditions at the left end (the presence of the spin 1) and free boundary conditions at the right end. The ground state of the chain is mainly determined by the left end. This can be seen from the fact that drastical changes in J_{end} hardly influence $\langle S_i^z \rangle$ even at the right end of the chain. The nonzero S_{total}^z expectation value is therefore communicated from the left end towards the right end by correlations, which we are partially neglecting due to the finiteness of M . On truncation, we systematically neglect states where the half-chains have high total $|S^z|$; this implies that $|S^z|$ values are reduced while their value is transmitted through the chain. To conserve S_{total}^z of the chain, each single $|S^z|$ is overestimated to make good this effective reduction. The smaller M , the more the absolute value of S^z is overes-

TABLE X. Average value $\langle |S_1^z| \rangle$ for the first spin of an $S=2$ chain with an effective free spin-1 at one end, in the ground state with $S_{\text{total}}^z = 1$.

M	$P(M)$	$\langle S_1^z \rangle$
50	0.14×10^{-4}	1.1924
74	0.37×10^{-5}	1.1709
95	0.15×10^{-5}	1.1552
126	0.61×10^{-6}	1.1420
150	0.26×10^{-6}	1.1376
180	0.16×10^{-6}	1.1334
∞	0	1.13(1)

timated, as we observe numerically. As the spin values are effectively fixed by the left chain end, the overestimation effect becomes increasingly important towards the right end, because more truncations have taken place.

To derive ξ , we give in Fig. 6 the local decay length $2/(\ln|S_i^z| - \ln|S_{i+2}^z|)$ (averaged over two neighboring sites to reduce odd-even site oscillations). One sees that at the spin-2 end of the chain, the correlation length is first rather short, but saturates to its bulk value (the shoulder). For $M=180$, the convergence of ξ for $M \rightarrow \infty$ can be well established, and we find a correlation length $\xi=49(1)$ in a system which has thus length $L \approx 5.5\xi$, which is consistent with minor finite size effects. At the same time, we find that $\langle S_1^z \rangle$ converges towards 1.13(1), supporting the picture of an effective free spin 1 at the end of the chain. The result is not very sensitive to M , as can be seen in Table X. For the calculation of the correlation length the question naturally arises whether we are really calculating the bulk correlation length when we are regarding a decay which is due to a particular end state of the chain. To investigate this question, we varied the coupling between the first spin (the effective free spin 1) and the second spin. We found that there is considerable variation of the S^z expectation value for the first few spins, whereas the correlation length remains (for our precision) unaffected, which we consider to support our claim that actually the bulk correlation length is calculated. This can be understood by considering the two limits of a very strong and very weak antiferromagnetic coupling of the first spin to the chain: For a very strong coupling, the first and second spin will form a singlet than cannot be excited ($\langle S_1^z \rangle = 0$); effectively the chain is shortened by 2, and we obtain the unmodified chain from site 3 onwards which will show the decay behavior described above. For the shortened chain, we will observe a small increase in $|\langle S_i^z \rangle|$, as the decay curve is shifted.

In the other limit, the first spin will be weakly linked to a chain which has total spin 1; the spin plus chain compound will also have total spin 1. Calculating the $S_{\text{total}}^z = 1$ ground state of the compound system, one sees that $\langle S_1^z \rangle = 1.5$, the maximum value $\langle S_1^z \rangle$ can obtain in the system under study. The chain will again be like an unmodified chain shortened by one site, showing the observed decay behavior and decay length, whereas the $|\langle S_i^z \rangle|$ will be reduced: the shortened chain is not in a $S_{\text{tot}}^z = 1$ state; one finds $S_{\text{tot}}^z = -0.5$. We are dealing with a superposition of the three degenerate ground states of the chain, which show all the same correlation

length. We have observed this increase of $\langle S_1^z \rangle$ and decrease of $\langle S_i^z \rangle$ ($i \geq 2$) for reduced couplings numerically.

The free spin-1 picture is therefore consistent with the fact that the decay length is unaffected by changes in the first coupling, but that $\langle S_1^z \rangle$ can be tuned continuously. The value 1.13(1) is just valid for an open chain with constant couplings; a similar argument holds of course for the value 0.53(1) given for the ends of open $S=1$ chains by White;^{14,15} here the minimum value is also 0, the maximum value 2/3.

Our correlation length [$\xi^{-1} \approx 0.0204(4)$] deviates seriously from the estimate $\xi^{-1} = 0.012(2)$ given by Hatano and Suzuki.³⁰ We think that this difference is due to the fact that the DMRG is much more suited to extract the correlation length than a quantum Monte Carlo algorithm.

VI. HIDDEN TOPOLOGICAL ORDER AND THE ROLE OF ANISOTROPIES

A. Hidden order in the isotropic chain

In the $S=1$ chain it is known that there is a hidden topological long-range order that is revealed in a nonlocal string correlation function. This order is simply understood in the surface language of Ref. 8. In the Haldane phase the antiferromagnetism is diluted in the following sense: the values $S^z = \pm 1$ alternates in a strict antiferromagnetic as one moves along the chain but an arbitrary number of values $S^z = 0$ may appear between nonzero values. This can be measured by the following correlation function:

$$G_\pi(m, n) = \left\langle S_m^z \exp \left[i\pi \sum_{k=m+1}^{n-1} S_k^z \right] S_n^z \right\rangle. \quad (13)$$

The order parameter is thus $\lim_{|n-m| \rightarrow \infty} G_\pi(n, m) = O_\pi$. It is related to the breakdown of a $Z_2 \times Z_2$ symmetry which is also nonlocal.¹⁰ This nonlocal symmetry cannot be extended straightforwardly to higher-spin chains. This is easily seen from the ground state degeneracy of open chains. An open VBS spin- S chain has exactly $(S+1)^2$ ground states due to the $S/2$ free spins at the end. For the $S=1$ chain, the *four* ground states are related by the operations of the $Z_2 \times Z_2$ group. The spontaneous breakdown of $Z_2 \times Z_2$ cannot however explain the $(S+1)^2$ degeneracy when $S > 1$. Nevertheless, the VBS wave functions do have a hidden topological long-range order for all integer spins: in the surface language, the spin- S wave function has a height that varies at most by S steps. This can be measured by the following correlation:

$$G_{\pi/S}(m, n) = \left\langle S_m^z \exp \left(i(\pi/S) \sum_{k=m+1}^{n-1} S_k^z \right) S_n^z \right\rangle. \quad (14)$$

Calculations by Refs. 31 and 32 indicate that $\lim_{|n-m| \rightarrow \infty} G_{\pi/2}(n, m) = O_{\pi/2}$ is nonzero for the $S=2$ spin chain. For the Affleck-Kennedy-Lieb-Tasaki (AKLT) model it is easily shown that $O_{\pi/2} = -1$ in the thermodynamic limit. For the numerical calculation of the parameter $O_{\pi/2}$ for the isotropic Heisenberg chain, one has to extrapolate, in analogy to the gap and the correlation length, in M and L . We have studied several systems, up to $M=150$ and $L=270$. We find that contrary to the case of the correlation length, the convergence in M is good and allows for an es-

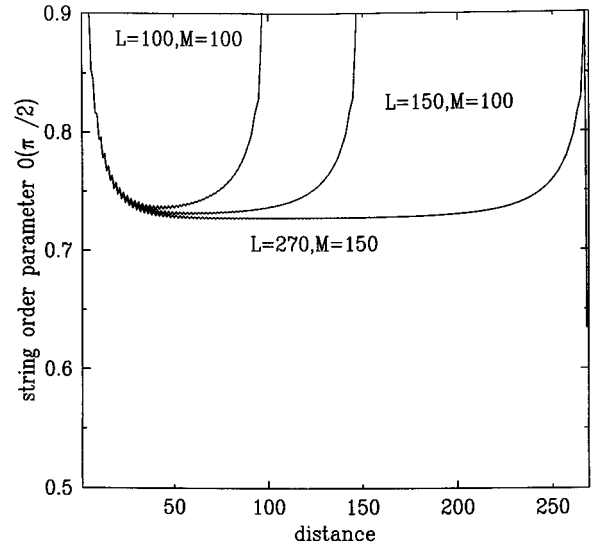


FIG. 7. Absolute value of the $S=2$ string order parameter for the isotropic Heisenberg chain for various L and M . The flat curve for $L=270$ shows that this order parameter is long range.

timation of the exact value better than 1%. Since this quantity $O_{\pi/2}$ is not simply related to the breakdown of a discrete symmetry $Z_2 \times Z_2$, contrary to the spin $S=1$ case, it is not clear in what sense it is an order parameter. This is what we investigate here.

In Fig. 7, we show our results for $M=100$, $L=100$; $M=100$, $L=150$; and $M=150$, $L=270$. We find that the effect of L and M finite is in both cases an overestimation of $O_{\pi/2}$. The overestimation due to the finite size is easily explained: the correlations fall for large distances, before rising again for $|i-j| \rightarrow L$: this is the effect of the boundary conditions; whereas the added boundary spins are not directly correlated, they effectively have partially the effect of periodic boundary conditions, as they force into the same end states. This gives a close resemblance to a periodic system, where the string order parameter is symmetric around $L/2$. The string order diminishes with M , as more fluctuations are taken into account. We find that $O_{\pi/2}$ has reached its thermodynamic limit for $L=270$. There is a nonzero expectation value, which we estimate from the behavior in M as $O_{\pi/2} = -0.726(2)$. The nonlocal order is thus common to the VBS wave function and the ground state of the Heisenberg $S=2$ chain.

B. The role of anisotropies

The hidden order can be destroyed in several ways: it can be replaced by an antiferromagnetic Ising order, by introducing an Ising anisotropy $J^z > 1$, and by a so-called large- D phase, where $S_i^z = 0$ for all i in the limit of $D \rightarrow \infty$, by introducing an anisotropy $D(S_i^z)^2$, $D > 0$. The anisotropic Hamiltonian is then

$$H = \sum_i S_i^x S_{i+1}^x + S_i^y S_{i+1}^y + J_z S_i^z S_{i+1}^z + D \sum_i (S_i^z)^2. \quad (15)$$

For $S=1$, the phase diagram with these two anisotropies is well known.⁸ We now discuss the corresponding $S=2$ phase diagram and the behavior of the string order parameter.

For $S > 1$, a bosonization study indicates³³ that there is a transition from a gapped Haldane phase to a gapped large- D phase qualitatively similar to the $S=1$ case. On the other hand, Oshikawa¹² has conjectured that there might be a cascade of S transitions in general. He proposes that by increasing D , successively the values $S_i^z = \pm S$, $S_i^z = \pm(S-1)$ and so on are suppressed. In the VBS picture, this corresponds to a successive dissolution of singlet bonds with $d/2+n=S$, with N the number of remaining singlet bonds between two sites, and n the number of spins $1/2$ on every site without bond, that form symmetrized states with total magnetization 0. One might therefore expect a cascade of S transitions to the large- D phase: each transition will be described by a change of the behavior of O_π : for n odd, it is nonzero in the thermodynamic limit, for n even, it is zero. Such a cascade of transitions has already been proposed by Affleck and Haldane³⁴ for the dimerization of chains. For the special case $S=2$, a suppression of $S_i^z = \pm 2$ (for $J^z=1$) would effectively lead, because of the transition elements for S^\pm , to an effective $S=1$ Hamiltonian with Ising anisotropy. Following Ref. 8, this $S=1$ Hamiltonian should be in the Haldane phase, supposing that the D that suppresses $S_i^z = \pm 2$ is still sufficiently small not to place this Hamiltonian directly into the large- D phase for $S=1$. One should therefore find a nonvanishing string order parameter O_π , whereas it vanishes for the original chain for $D=0$.

As we do not know which phases to expect, it is essential to prepare the open spin-2 chain such that the low-lying excitations are bulk excitations (see the discussion above) and end artefacts eliminated. We attach two spins 1 to the chain ends, to eliminate the degeneracy of the ground state in the Haldane phase. As we have seen, the end coupling J_{end} must be sufficiently strong to push the energy costs of an edge excitation beyond that of the lowest bulk excitation. For large D , one expects a gap of the order D between ground and first excited state. J_{end} must therefore be chosen on this scale, as we know nothing *a priori* on the ground state of the chain as a function of D . We will see that the system tries to minimize the gap by giving antiferromagnetic energy to compensate the energy cost caused by D . A strong end coupling contains a lot of compensation energy, and has thus a tendency to localize the excitation in the ends. It is therefore also necessary to increase the cost of an edge excitation due to D by increasing D on the end sites. We have chosen $D_{\text{end}} \approx 20D$ on the two first and last sites. To check whether these manipulations are sufficient to obtain the bulk excitations, we have calculated $\langle S_i^z \rangle$ for the first excitation given by $S_{\text{total}}^z = \pm 1$, and checked that the excitation is not localized on the ends, which would be indicated by a strong increase of $\langle S_i^z \rangle$ towards the ends. All results given below are bulk results.

We have calculated the gap, the spin-spin correlations and the string correlation functions O_π and $O_{\pi/2}$ as well as the truncation error for $0 \leq D \leq 6$. To calculate the gap, we consider chains up to $L=120$ and keep $M=110$ states. For an isotropic chain, the first excitation (total spin 1) is a degenerate triplet. In the presence of an anisotropy $D \neq 0$, this degeneracy is lifted: one obtains a doublet $S_{\text{total}}^z = \pm 1$ and a singlet $S_{\text{total}}^z = 0$. The doublet is lower in energy than the singlet for $D > 0$ (and inversely for $D < 0$).³⁵ For $D > 0$ the gap

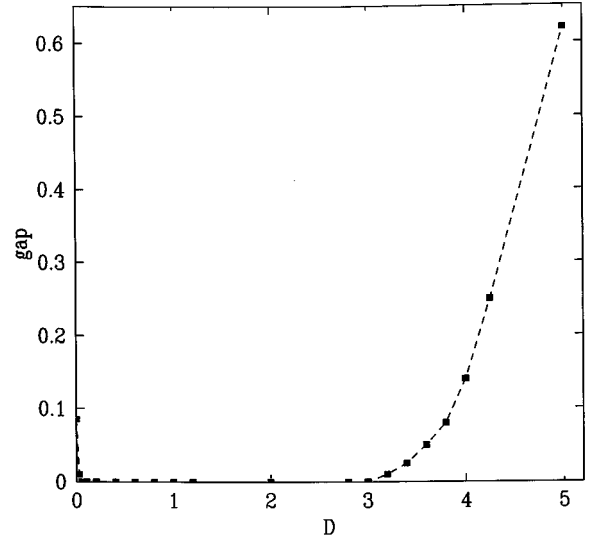


FIG. 8. Gaps for the $S=2$ Heisenberg chain with single-ion easy-plane anisotropy D .

can therefore be calculated by taking the energy difference between the ground states for $S_{\text{total}}^z=0$ and $S_{\text{total}}^z=1$; for $D < 0$, one has to take the difference between the first two states with $S_{\text{total}}^z=0$.

We find the gap behavior shown in Fig. 8. For $D=0.025$ the correlation length is already very large. A L^{-1} extrapolation gives us a lower bound, which is nonzero; due to the relatively small slope of the gap curve, we have taken this value as gap estimation. For $0.05 < D < 3.0$ we find gap curves that do not show a systematic deviation from the L^{-1} behavior as in Fig. 5, though the truncation error was rather large (10^{-8}). This is due to the fact that the truncation errors associated with the two energies are nearly identical and the systematic errors thus largely compensate. An extrapolation in L^{-1} towards $L \rightarrow \infty$ seems thus permitted, and gives vanishing gaps in the whole regime. By taking the gap obtained for $L=120$ as the thermodynamic limit, which gives a seriously overestimated result, we obtain in the whole region upper bounds of the order of 0.02. For $D > 3.0$, a gap develops, the correlation lengths become increasingly short and the truncation error diminishes by several orders of magnitude. The gap estimations become again very precise. We find thus a gap for very small D : it vanishes for $0.025 < D < 0.05$. We find then a rather large *critical* phase, terminating at $D=3.0(1)$. The system is then gapped, with a small growth of the gap just above $D=3.0$. These results are surprising; they indicate that there is a whole critical phase between the Haldane and the large- D phase, whereas there was just a single critical point³⁵ for $S=1$, as predicted by bosonization.³⁵ Of course, these results are within our actual precision and we do not expect simple gap scaling to give precise phase boundaries.

We have no indication of a degeneracy of the ground state in the critical phase, which could then exhibit a gapped spectrum despite our results. The indirect indications that the phase is truly critical are very strong: the truncation error diminishes slowly with D , but remains rather large, whereas it diminishes quickly as soon as the gap sets in. Our other calculations indicate that a simple degeneracy of the ground

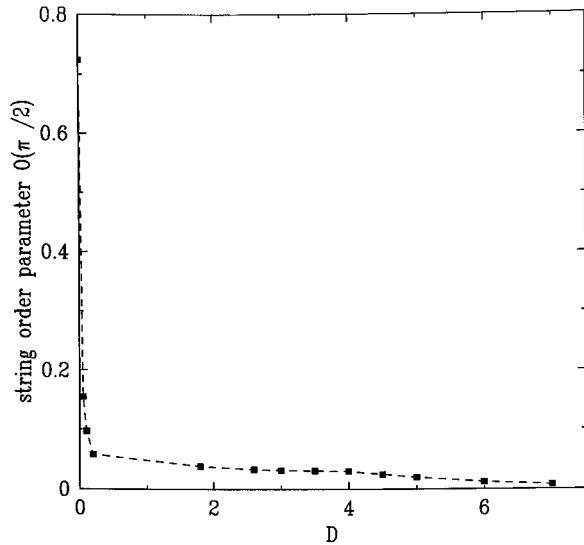


FIG. 9. $S=2$ string correlation function $O_{\pi/2}$ for the Heisenberg chain vs single-ion easy-plane anisotropy D .

state in a gapped spectrum does not lead to a big increase in the truncation error: the DMRG chooses quickly one of those states and ignores the others. A more physical and stronger argument is given by the very slow decrease of the spin-spin correlations, which also indicates the presence of a critical phase. Correlation lengths we estimated on system lengths $L=150$ were systematically bigger than the system size.

C. Hidden order in the large- D phase

We now turn to the string correlation functions O_π and $O_{\pi/2}$. We find for all D that the long-range expectation value of O_π is always less than 10^{-4} to 10^{-5} for distances ≈ 150 . The presence of an intermediate phase with the characteristics as predicted by Oshikawa¹² seems therefore excluded. The situation is completely different for $O_{\pi/2}$ (Fig. 9). We find that for all D it has a nonvanishing thermodynamic limit, which goes to 0 monotonically for $D \rightarrow \infty$. The slope is very large for small D : for $D=0.2$, $O_{\pi/2}$ is less than 10% of the $D=0$ value. The analysis of $O_{\pi/2}$ is different in the various phases: it is very easy for the large- D phase, where the small truncation error makes the results very precise and where the short correlation length assures a fast convergence to the thermodynamic limit. The values thus obtained have a relative precision of at least 10^{-4} , and there is thus no doubt that $O_{\pi/2}$ is nonzero in the large- D phase and vanishes only in the $D \rightarrow \infty$ limit.

In the critical phase, the analysis is more complicated due to the relatively large truncation errors (10^{-8}), but mainly because of the power-law correlations: the thermodynamic limit has not yet been reached for the lengths we consider. We find that our results can be reasonably extrapolated in this regime as L^{-1} , and that the effects of M finite are relatively small for the M considered. It cannot be excluded however that $O_{\pi/2}$ decays algebraically to zero in this intermediate phase. Since we have good evidence that $O_{\pi/2}$ is nonzero for D large enough, we consider this possibility as unlikely. We conclude that $O_{\pi/2}$ is not an order parameter in the sense that it is not zero in the thermodynamic limit for

the large- D phase (it is not zero either in an antiferromagnetically ordered phase, but becomes zero, if the antiferromagnetic order parameter is subtracted). This quantity cannot discriminate between the Haldane and the large- D phase.

D. The $S=2$ phase diagram

Finally we have mapped out the boundaries of the XY critical phase by adding also exchange anisotropy. We find that the critical phase extends to the Ising AF phase that appears when J_z is large enough. To the precision of our measurements, we find that the Haldane phase is confined in a narrow region around the isotropic point: see Fig. 3 of Ref. 13. We have performed 20 measurements to fix the boundaries of the Haldane phase which is the most crucial. There are five measurement points on the line between XY and the ferromagnetic phase and also five points on the line between the large- D and the XY phases. Bosonization predicts³³ that there are *two* XY phases separated by an Ising transition: these phases differ by the way spin correlations decay. Since we measured gaps to locate the phase boundaries, we cannot discriminate between these two phases. The phase diagram we find is a topological distortion of the bosonization result. This distortion is a large one and brings the system closer to the classical limit. Indeed, when $S \rightarrow \infty$, the phase boundaries are straight lines: $1+D=J_z$ ($-J_z$) for $J_z > 0$ ($J_z < 0$) between XY and AF (F) and the vertical axis $J_z=0$ between F and AF. This is already very close to Fig. 3 of Ref. 13, simply the Haldane and large- D phase have to disappear. This suggests that the S - XY boundary will be pushed to infinity when $S \rightarrow \infty$ and the Haldane region becomes increasingly smaller, collapsing around the isotropic point since the Haldane gap vanishes exponentially $\Delta \approx \exp[-\pi S]$ and is thus easier to destroy. We thus suggest that the phase diagram for $S=2$ is generic for higher spins, contrary to the peculiar case of $S=1$.

VII. CONCLUSION

We have established numerical values for the gap and correlation length of the isotropic Heisenberg $S=2$ spin chain, in agreement with the Haldane conjecture. We have measured a nonlocal parameter inspired by the VBS wave function and shown that it is nonzero in the Haldane phase. We have also studied single-ion and exchange anisotropies. The corresponding phase diagram is topologically different from that of spin 1 and leads to a simple conjecture about the classical limit. The nonlocal string order parameter is nonzero in the whole Haldane phase but also at least in the large- D phase and most likely in the XY phase: it is not a good order parameter to discriminate between these phases.

Finally we give simple arguments to interpret the phase diagram. There is a critical anisotropy D_{c_1} limiting the Haldane phase when D increases from zero. For $S=2$, $0.025 < D_{c_1} < 0.05$. Its value is ruled by the value of the Haldane gap for $D=0$. The gap energy is balanced by the anisotropy D energy, which is of the order $D[S^2 - (S-1)^2] = D(2S-1)$. We therefore estimate $D_{c_1} \approx \Delta_S/S$. As $\Delta_S \rightarrow 0$ for $S \rightarrow \infty$, D_{c_1} diminishes monotonously with S and is zero in the classical limit. There is also a critical anisotropy D_{c_2} that limits the large- D phase from

the large- D limit. To estimate D_{c_2} , we consider the limit $D \rightarrow \infty$. In that limit, the ground state is given by $S_i^z = 0$ on all sites i and energy 0. The first excitation is constructed by putting $S_i^z = \pm 1$ on one site. These spin flips disperse in a band due to the exchange term. A first-order perturbation calculation from the $D = \infty$ limit gives the dispersion

$$E(k) = D + JS(S+1)\cos k. \quad (16)$$

The gap is thus $D - JS(S+1)$. We estimate D_{c_2} by the condition that the gap vanishes and $D_{c_2} \approx S(S+1)$: this is the softening of the excitations. We thus find $D_{c_1} = 2$ and $D_{c_2} = 6$ for $S=1$ and $S=2$, to be compared to the numerical values 0.99(1) and 3.0(1). We overestimate D_{c_2} , but seem to capture the essential; a more involved perturbation calculation³⁶ does not change anything fundamental. For $S \rightarrow \infty$, $D_{c_2} \rightarrow \infty$: the large- D phase disappears. Let us point out that these arguments in fact give immediately the classi-

cal limit: $D_{c_1} = 0$ and $D_{c_2} = \infty$; the system is always critical. For $D > 0$, the system exhibits a spectrum without gap: the spins are in the XY plane.

Nothing in these arguments introduces a difference between different sorts of spins for $S \geq 2$. We conjecture therefore, that for $S \geq 2$ the Haldane phase and the large- D phase are separated by a critical phase, whose lower limit tends to $D=0$ for $S \rightarrow \infty$ and is essentially determined by the Haldane gap, whereas the upper limit tends to $D = \infty$ for $S \rightarrow \infty$ and is essentially determined by $\approx S^2$. The $S=1$ case therefore appears as a special case: $D_{c_1} = D_{c_2}$. We note that the phase diagram we have proposed is in agreement with an earlier proposal of Khveshchenko and Chubukov.³⁷

ACKNOWLEDGMENTS

It is a pleasure to thank N. Elstner, D. Huse, and R. Lacaze for useful discussions.

-
- ¹F. D. M. Haldane, Phys. Lett. **93A**, 464 (1983); Phys. Rev. Lett. **50**, 1153 (1983).
²R. Botet and R. Jullien, Phys. Rev. B **27**, 613 (1983).
³R. Botet, R. Jullien, and M. Kolb, Phys. Rev. B **28**, 3914 (1983).
⁴J. B. Parkinson and J. C. Bonner, Phys. Rev. B **32**, 4703 (1985).
⁵M. P. Nightingale and H. W. J. Blöte, Phys. Rev. B **33**, 659 (1986).
⁶M. Takahashi, Phys. Rev. B **38**, 5188 (1988); K. Nomura, *ibid.* **40**, 2421 (1989); S. Liang, Phys. Rev. Lett. **64**, 1597 (1990); K. Kubo, Phys. Rev. B **46**, 866 (1992).
⁷I. Affleck, T. Kennedy, E. H. Lieb, and H. Tasaki, Phys. Rev. Lett. **59**, 799 (1987); Commun. Math. Phys. **115**, 477 (1988).
⁸M. den Nijs and K. Rommelse, Phys. Rev. B **40**, 4709 (1989).
⁹S. M. Girvin and D. P. Arovas, Phys. Scr. T **27**, 156 (1989).
¹⁰T. Kennedy and H. Tasaki, Phys. Rev. B **45**, 304 (1992).
¹¹H. Q. Lin, Phys. Rev. B **42**, 6561 (1990).
¹²M. Oshikawa, J. Phys.: Condens. Matter, **4**, 7469 (1992).
¹³U. Schollwöck and Th. Jolicœur, Europhys. Lett. **30**, 493 (1995).
¹⁴S. R. White and R. M. Noack, Phys. Rev. Lett. **68**, 3487 (1992); S. R. White, *ibid.* **69**, 2863 (1992); Phys. Rev. B **48**, 10345 (1993).
¹⁵S. R. White and D. A. Huse, Phys. Rev. B **48**, 3844 (1993).
¹⁶E. S. Sørensen and I. Affleck, Phys. Rev. Lett. **71**, 1633 (1993).
¹⁷D. P. Arovas, A. Auerbach, and F. D. M. Haldane, Phys. Rev. Lett. **60**, 531 (1988).
¹⁸J. Deisz, M. Jarrell, and D. L. Cox, Phys. Rev. B **48**, 10227 (1993).
¹⁹Y. Nishiyama, K. Totsuka, N. Hatano, and M. Suzuki, J. Phys. Soc. Jpn. **64**, 414 (1995).
²⁰O. Golinelli, Th. Jolicœur, and R. Lacaze, Phys. Rev. B **45**, 9798 (1992).
²¹H. W. J. Blöte, Physica B **93**, 93 (1978).
²²M. Kolb, R. Botet, and R. Jullien, J. Phys. A **16**, L673 (1983).
²³Y. Hatsugai, J. Phys. Soc. Jpn. **61**, 3856 (1992).
²⁴O. Golinelli, Th. Jolicœur, and R. Lacaze, Phys. Rev. B **50**, 3037 (1994).
²⁵M. P. Nightingale, in *Finite Size Scaling and Numerical Simulations of Statistical Systems*, edited by V. Privman (World Scientific, Singapore, 1990).
²⁶J. H. Hetherington, Phys. Rev. A **30**, 2713 (1984).
²⁷N. Cerf and O. C. Martin, Phys. Rev. E **51**, 3679 (1995).
²⁸M. P. Nightingale and H. W. J. Blöte, Phys. Rev. Lett. **60**, 1562 (1988).
²⁹E. Granato and M. P. Nightingale, Phys. Rev. B **48**, 7438 (1993).
³⁰N. Hatano and M. Suzuki, J. Phys. Soc. Jpn. **62**, 1346 (1993).
³¹Y. Hatsugai, J. Phys. Soc. Jpn. **61**, 3856 (1992).
³²K. Totsuka and M. Suzuki, J. Phys.: Condens. Matter **7**, 1639 (1995).
³³H. J. Schulz, Phys. Rev. B **34**, 6372 (1986).
³⁴I. Affleck and F. D. M. Haldane, Phys. Rev. B **36**, 5291 (1987).
³⁵O. Golinelli, Th. Jolicœur, and R. Lacaze, Phys. Rev. B **46**, 10854 (1992).
³⁶N. Papanicolaou and P. Spathis, J. Phys.: Condens. Matter **1**, 5555 (1989); **2**, 6575 (1990).
³⁷D. V. Khveshchenko and A. V. Chubukov, Sov. Phys. JETP **66**, 1088 (1987).